

A systematic multiscale modeling and experimental approach to understand corrosion at grain boundaries in magnesium alloys

PI: Mark Horstemeyer

Graduate Students: Weiwei Song, Nitin Sukhija

Center for Advanced Vehicular Systems

Mississippi State University

Co-PI: Santanu Chaudhuri

Postdoc Researcher: Aslihan Sumer

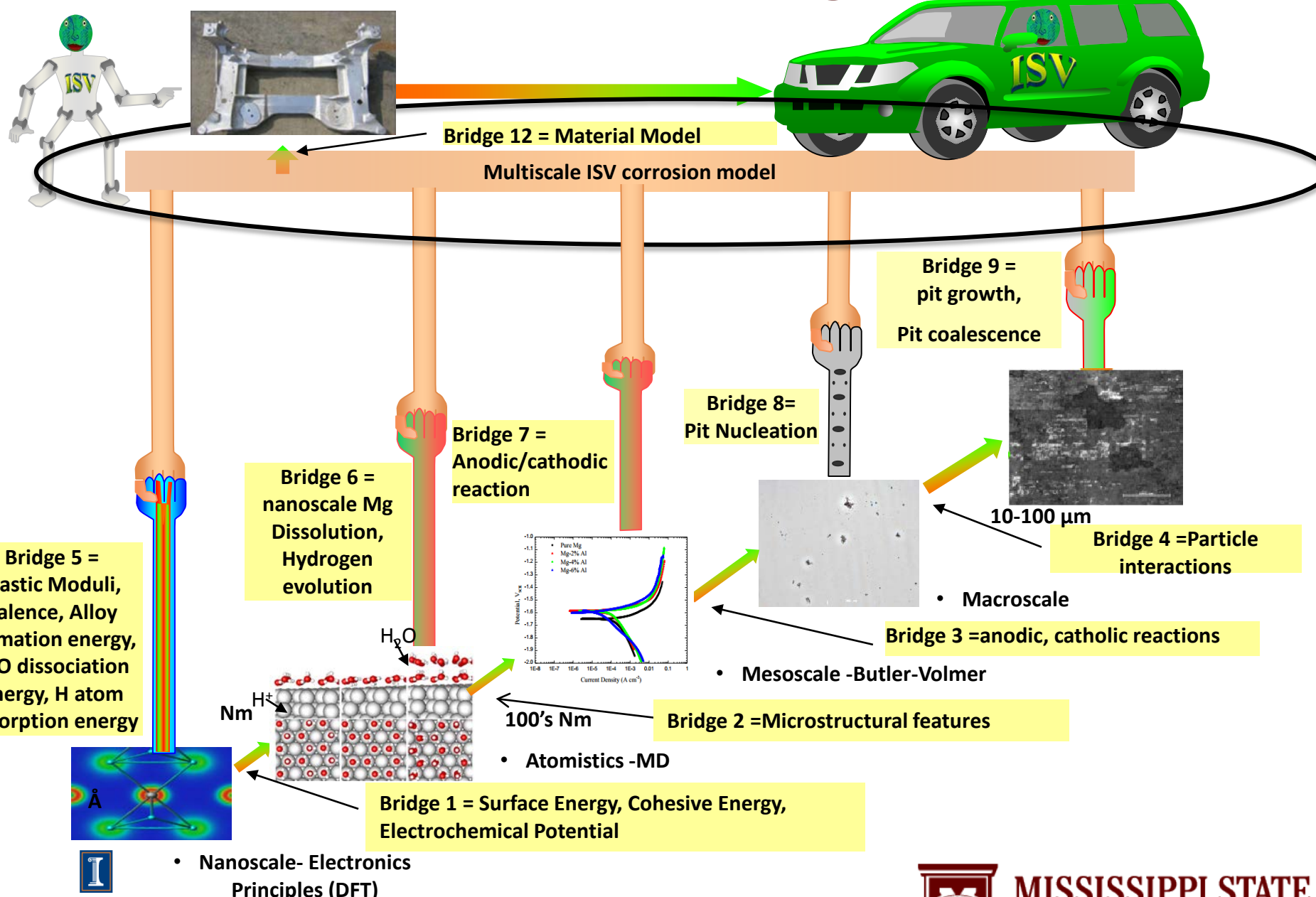
The Illinois Applied Research Institute

University of Illinois at Urbana-Champaign

Project ID: LM095

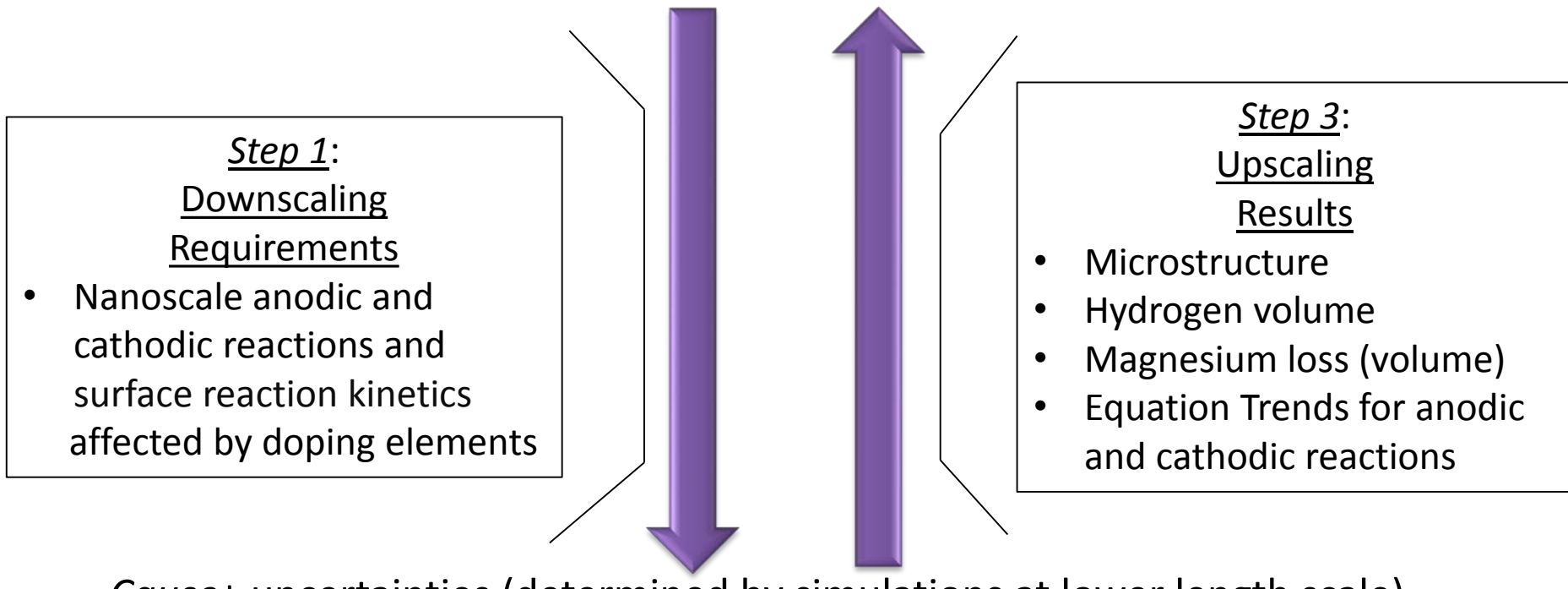
- Why Use Magnesium
 - Lightweight to replace heavy engine parts
 - High stiffness to weight ratio
 - High strength to weight ratio
 - Excellent castability and damping capacity
 - Easily corroded in the presence of salt-water
- Why ICME and Multiscale Modeling
 - Reduce product development time
 - Reduce product costs through innovation in material, product, and process designs
 - Reduce the number of costly large systems scale experiments
 - Increase product quality and performance by providing more accurate predictions of response to design loads
 - Help develop new materials

Multiscale Corrosion Modeling



Multiscale Corrosion Internal State Variable (ISV) model

Effect: Macroscopic Corrosion Damage (Electrochemical Potential, Hydrogen Evolution Rate, Anodic Dissolution Rate)



Step 2: Simulation at NanoScale (DFT) and Atomics scale (MD)

- Effect of doping on surface stability
- Adsorption energies of molecules relevant to corrosion
- Identify the role of cathodic impurities (elements) vs cathodic precipitates (phases)
- Water dissociation reactions
- Mg dissolution reactions
- Hydrogen evolution reactions

Outline

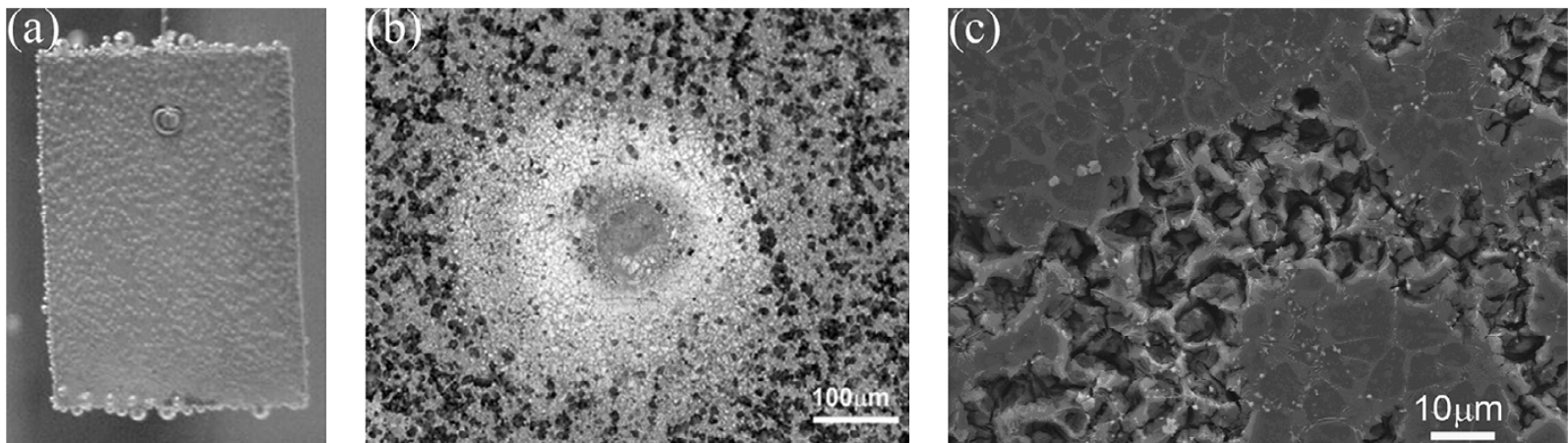
- Macroscale Corrosion Damage Framework
- Mesoscale Corrosion Modeling
- Nanoscale Corrosion Simulation
- Experiment Calibration
- Application and Implementation

What is an Internal State Variable (ISV) ?

- Uniquely defines the Helmholtz (or Gibbs) free energy of a system undergoing an **irreversible process**
- Describes the **internal structure rearrangement** with the associated length scales
- Selection is arbitrary, but the rate equations are **physically motivated (microstructural morphology)** and strongly **influence the history** of the material and can be garnered from lower length scale arguments

Kinetics of Plasticity-Damage-Corrosion Framework

- Corrosion Damage



Macroscopic observation examples of the (a) general, (b) pitting, and (c) intergranular damage mechanisms on specimen surfaces (Alvarez et al., 2010)

$$\phi_c = \phi_{gc} + \phi_{pc} + \phi_{ic}$$
$$\dot{\phi}_{total} = \dot{\phi}_{gc} + \dot{\phi}_{pc} + \dot{\phi}_{ic}$$
$$\phi_{pc} = \eta_p v_p c_p$$
$$\dot{\phi}_{pc} = \dot{\eta}_p v_p c_p + \eta_p \dot{v}_p c_p + \eta_p v_p \dot{c}_p$$

C.A. Walton, M.F. Horstemeyer, H.J. Martin, D.K. Francis, Formulation of a macroscale corrosion damage internal state variable model, International Journal of Solids and Structures, 51 (2014) 1235-1245.

Macroscale-Mesoscale Bridge Information

Macroscale : Internal State Variable Theory

$$\dot{\phi}_{total} = \dot{\phi}_{gc} + \dot{\phi}_{pc} + \dot{\phi}_{ic}$$

$$\dot{\phi}_{gc} = \frac{C_1 M}{F_Z} (C_2 - \phi_{gc})$$

$$\dot{\eta} = \begin{cases} C_3(C_4 - \eta) & \text{if } t < t_{critical} \\ C_5(C_6 - \eta) & \text{if } t \geq t_{critical} \end{cases}$$

$$\dot{\phi}_{pc} = \dot{\eta}_p v_p c_p + \eta_p \dot{v}_p c_p + \eta_p v_p \dot{c}_p$$

$$\dot{\phi}_{ic} = \begin{cases} C_{15}(C_{16} - \phi_{ic}) \left(\frac{MO}{MO_0} \right)^{z_{ic}} & \text{if } t < t_c \\ C_{17}(C_{18} + \phi_{ic}) \left(\frac{MO}{MO_0} \right)^{z_{ic}} & \text{if } t \geq t_c \end{cases}$$

$$\dot{v}_p = \begin{cases} C_7(C_8 - A) & \text{if } t < t_{critical} \\ C_9(C_{10} + A) & \text{if } t \geq t_{critical} \end{cases}$$

$$\dot{c}_p = \frac{k_e q_1 q_2}{\varepsilon_0 \pi (NND(t))^4}$$

Mesoscale : Butler-Volmer Equation

$$I = A \cdot j_0 \cdot \left\{ \exp \left[\frac{\alpha_a nF}{RT} (E - E_{eq}) \right] - \exp \left[-\frac{\alpha_c nF}{RT} (E - E_{eq}) \right] \right\}$$

I : electrode current

A : electrode active surface area

J : electrode current density

E : electrode potential

E_{eq} : equilibrium potential

α_c : cathodic charge transfer coefficient

α_a : anodic charge transfer coefficient

Outline

- Macroscale Corrosion Damage Framework
- Mesoscale Corrosion Modeling
- Nanoscale Corrosion Simulations
- Experiment Calibration
- Application and Implementation

Mesoscale Modeling/Simulations

$$I = A \cdot j_0 \cdot \left\{ \exp \left[\frac{\alpha_c nF}{RT} (E - E_{eq}) \right] - \exp \left[-\frac{\alpha_a nF}{RT} (E - E_{eq}) \right] \right\}$$

I : electrode current

A : electrode active surface area

J : electrode current density

E_{eq} : equilibrium potential

E : electrode potential



$\alpha_c = f(\text{second phase number density, second phase particle size, second phase nearest neighbor distance, matrix composition, solution type (water, salt water, etc.), and hydrogen evolution})$

$\alpha_a = f(\text{second phase number density, second phase particle size, second phase nearest neighbor distance, matrix composition, solution type (water, salt water, etc.), and magnesium dissolution rate})$

Outline

- Macroscale Corrosion Damage Framework
- Mesoscale Corrosion Modeling
- **Nanoscale Corrosion Simulations**
- Experiment Calibration
- Application and Implementation

Mesoscale-Nanoscale Bridge Information

Mesoscale : Butler-Volmer Equation

$$I = A \cdot j_0 \cdot \left\{ \exp \left[\frac{\alpha_a nF}{RT} (E - E_{eq}) \right] - \exp \left[- \frac{\alpha_c nF}{RT} (E - E_{eq}) \right] \right\}$$

I : electrode current

A : electrode active surface area

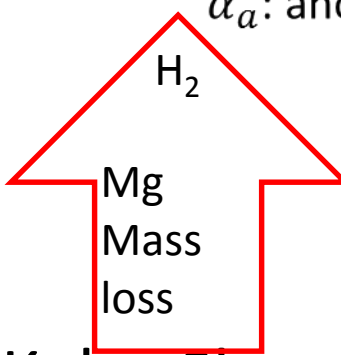
J : electrode current density

E : electrode potential

E_{eq} : equilibrium potential

α_c : cathodic charge transfer coefficient

α_a : anodic charge transfer coefficient



Nanoscale :Kohn-Sham Equations

$$E[\rho] = T_s[\rho] + \int d\mathbf{r} v_{ext}(\mathbf{r})\rho(\mathbf{r}) + V_H[\rho] + E_{xc}[\rho]$$

$$v_{eff}(\mathbf{r}) = v_{ext}(\mathbf{r}) + e^2 \int \frac{\rho(\mathbf{r}')}{|\mathbf{r} - \mathbf{r}'|} d\mathbf{r}' + \frac{\delta E_{xc}[\rho]}{\delta \rho(\mathbf{r})}.$$

$$T_s[\rho] = \sum_{i=1}^N \int d\mathbf{r} \phi_i^*(\mathbf{r}) \left(-\frac{\hbar^2}{2m} \nabla^2 \right) \phi_i(\mathbf{r}),$$

$$E = \sum_i^N \varepsilon_i - V_H[\rho] + E_{xc}[\rho] - \int \frac{\delta E_{xc}[\rho]}{\delta \rho(\mathbf{r})} \rho(\mathbf{r}) d\mathbf{r}$$

$$V_H = \frac{e^2}{2} \int d\mathbf{r} \int d\mathbf{r}' \frac{\rho(\mathbf{r})\rho(\mathbf{r}')}{|\mathbf{r} - \mathbf{r}'|}.$$

Background: Atomistic Framework

Oxide layer protection: Previous DFT investigation

- DFT Calculated Grain Boundary and bulk doping of MgO developed previously
- Rare-earth doping improve oxide layer stability¹
- Grain boundary segregated of species that bound water strongly are favorable
- Aggressive species interaction with oxide layer underway

Anodic dissolution and galvanic coupling to cathodic precipitates

- Anodic and cathodic reactions for corrosion progression in Mg-X alloys
- Alloying elements and surface reaction kinetics
- Connection to microstructure and cathodic precipitate distribution
- Multiscale connection to experiments and ISV model

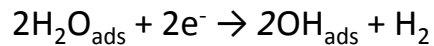
¹Kwak, Hyunwook, and Santanu Chaudhuri. "Cationic doping of MgO surfaces to build corrosion protection in Mg alloys." *Journal of Alloys and Compounds* 509.32 (2011): 8189-8198.

Corrosion Reactions in Mg-Alloys

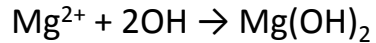
- Overall Reaction can be expressed as: $Mg + 2H_2O \rightarrow Mg(OH)_2 + H_2$
- Contributing half-cell reactions



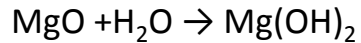
Anodic: Oxidation reaction



Cathodic: Reduction reaction

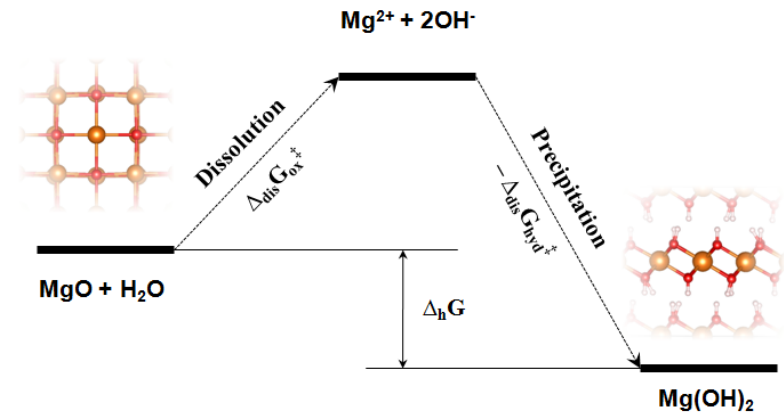
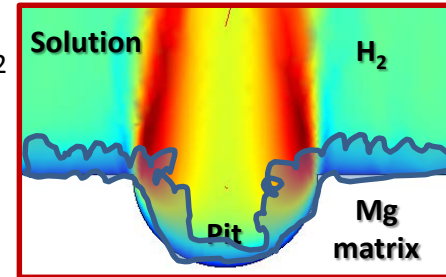


Corrosion product



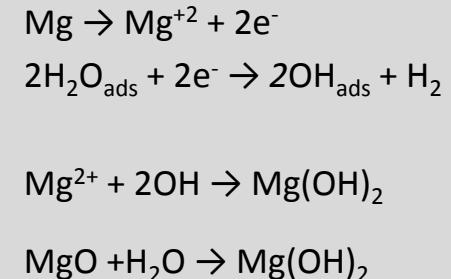
- Alloying elements Mg-X (X=Ca,Al,Mn,Fe,Zn,As..) change cathodic/anodic reactions
- Alloying element and segregation change $MgO \leftrightarrow Mg(OH)_2$ dissolution/precipitation/transport kinetics

		Elements and their Electronegativities																			
H	2.1																			He	-
Li	1.0	Be	1.5																	Ne	-
Na	0.9	Mg	1.2																	Ar	-
K	0.8	Ca	1.0	Sc	1.3	Ti	1.5	V	1.6	Cr	1.6	Mn	1.5	Fe	1.8	Co	1.8	Ni	1.8	B	2.0
Rb	0.8	Sr	1.0	Y	1.2	Zr	1.4	Nb	1.6	Mo	1.8	Tc	1.9	Ru	2.2	Rh	2.2	Pd	2.2	C	2.5
Ge	0.7	Ba	1.1-1.2	La-I.u		Hf	1.3	Ta	1.5	W	1.7	Re	1.9	Os	2.2	Ir	2.2	Pt	2.2	N	3.0
																			O	3.5	
																			F	4.0	
																			Cl	3.0	
																			Br	2.8	
																			Se	2.4	
																			In	1.7	
																			Sn	1.8	
																			Sb	1.9	
																			Te	2.1	
																			I	2.5	
																			Xe	-	
																			Po	2.0	
																			At	2.2	
																			Rn	-	



Kohn-Sham Eqtns used in Density Functional Theory (DFT) Calculations

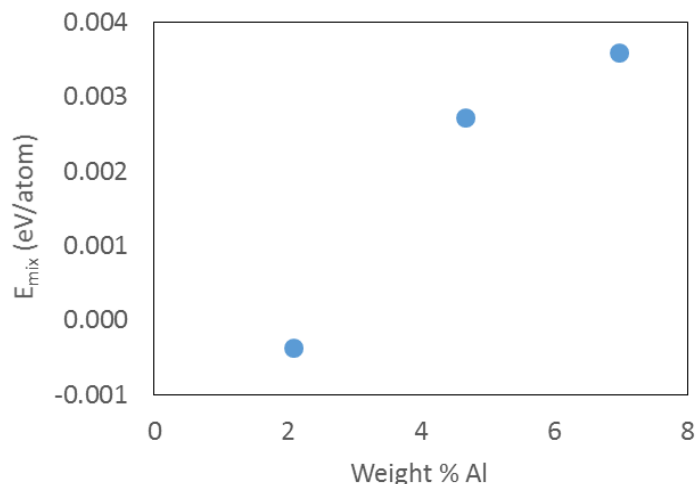
- Overall Reactions calculated using DFT methods on Mg(001) slab surface
- Alloying elements Mg-X (X=Ca,Al,Mn,Fe,Zn,As..) compared
- Focus on Mg-Al results for establishing understanding and baseline of corrosion rates
- Identify the role of cathodic sites (elements) vs cathodic precipitates (phases)



Less Al in preferred compared to higher Al% in terms of alloy formation energy

$$E_{\text{mixing}} = (E_{\text{total}} - n_{\text{Mg}}E_{\text{Mg(bulk)}} - n_{\text{Al}}E_{\text{Al(bulk)}})/(n_{\text{Mg}} + n_{\text{Al}})$$

Energy of Mg-Al Bulk System with Al at Different Concentrations



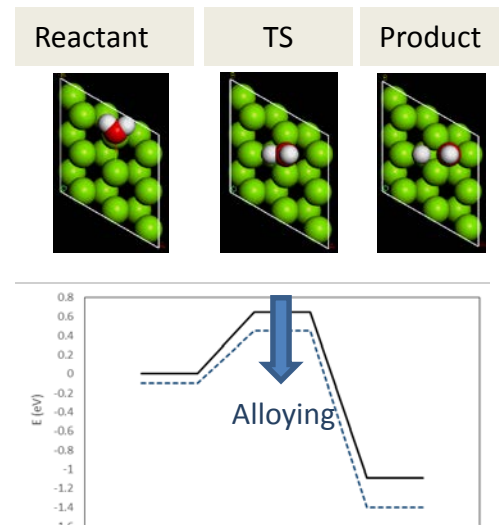
DFT Calculations for Water Dissociation Reactions

Show that as the %AL Increases the Barrier Energy Decreases

- Water transports through the MgO/Mg(OH)₂ layer and reacts with Mg-alloy matrix
- Al in-solution of Mg matrix and Mg₁₇Al₁₂ phase are investigated

Surface	$E_{\text{ads}, \text{H}_2\text{O}}$ (eV)	$E_{\text{ads}, \text{H}}$ (eV)	$E_{\text{ads}, \text{OH}}$ (eV)	ΔH_{Rxn} (eV) $\text{H}_2\text{O}_{\text{ads}} \rightarrow \text{OH}_{\text{ads}} + \text{H}_{\text{ads}}$	E_{Barrier} (eV) $\text{H}_2\text{O}_{\text{ads}} \rightarrow \text{OH}_{\text{ads}} + \text{H}_{\text{ads}}$
Pure Mg	-0.43	-2.38	-4.95	-1.09*	0.65
Mg-1Al	-0.50	-2.45	-5.01	-1.16	0.64
Mg-2Al	-0.54	-2.40	-5.10	-1.15	0.64
Mg ₁₇ Al ₁₂	-0.66	-2.52	-5.14	-1.20	0.62

$\Delta H_{\text{correction}}$: -0.17 $\Delta G_{\text{correction}}$: -0.04



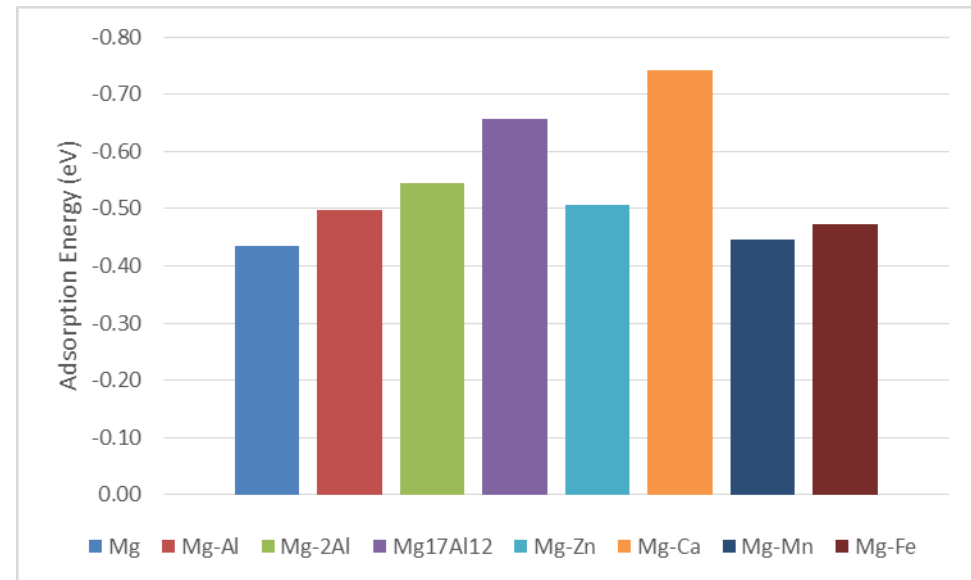
Barrier of H₂O dissociation more favorable for beta-phase Mg₁₇Al₁₂

H₂O/OH binds strongly but H adsorption shows trend reversal at higher Al concentration

Mg-X Alloys: Impurity Promotes Water Dissociation Reactions

Surface	E_{ads, H_2O} (eV)	$E_{ads,H}$ (eV)	$E_{ads,OH}$ (eV)	ΔH_{Rxn} (eV)
Pure Mg	-0.43	-2.38	-4.95	-1.09
Mg-Al	-0.50	-2.45	-5.01	-1.16
Mg-Zn	-0.51	-2.44	-5.04	-1.17
Mg-Ca	-0.74	-2.66	-5.19	-1.30
Mg-Mn	-0.45	-2.63	-4.95	-1.33
Mg-Fe	-0.47	-2.68	-4.98	-1.38

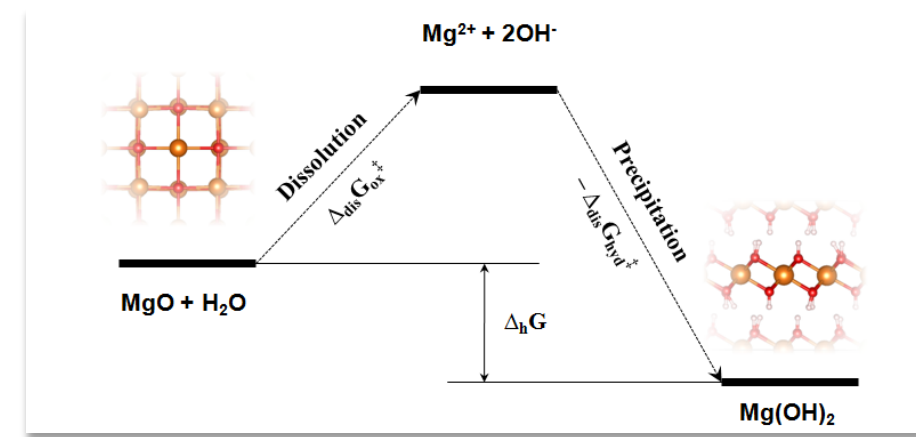
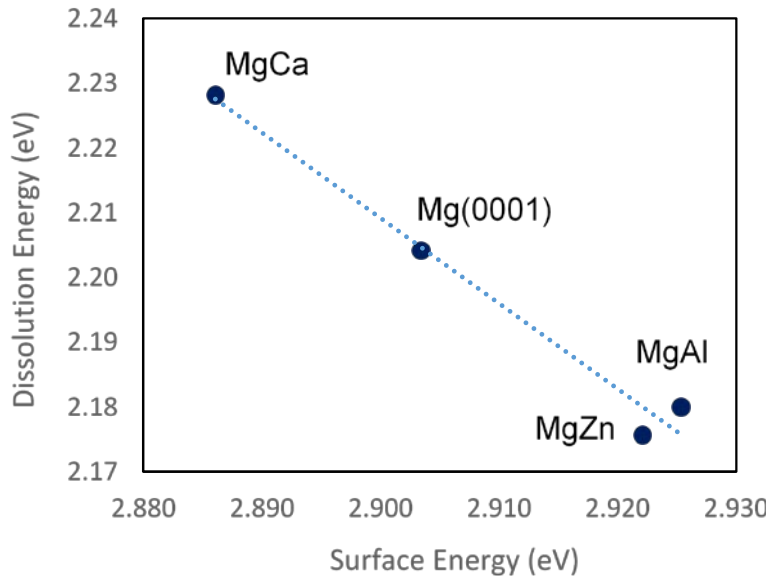
In general cathodic impurities promote water dissociation but also increase H adsorption.



Mg-X Alloys: Mg Dissolution Reactions

Defect formation energy is important since anodic dissolution is first step for metal loss and Mg(OH)_2 precipitation. Reaction happens at two interfaces:

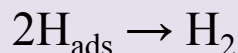
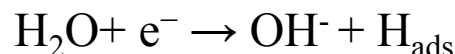
- On the $\text{MgO}/\text{Mg(OH)}_2$ interface
- At the metal layer/oxide/hydroxide layer – Mg(0001) used a guide for the trends



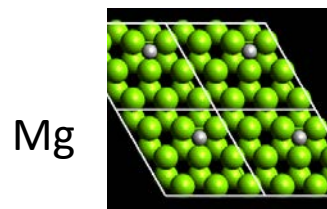
Barrier layer in Mg is ineffective – thus, anodic dissolution trend is determined by dissolution at the grain boundaries and from flat surfaces

Mg-Al Corrosion: H₂ Evolution Reaction Trend

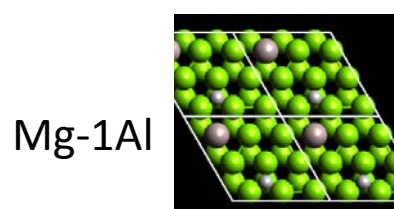
Cathodic Rxn's followed



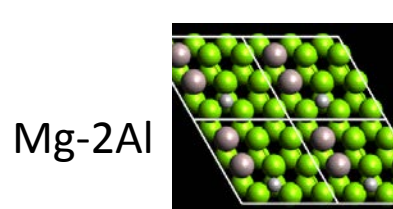
Reaction barrier (rate)
depend on H atom
adsorption energy



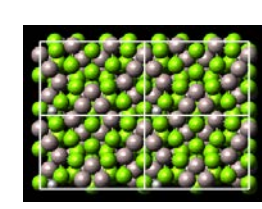
E_{ads} : -2.38 eV



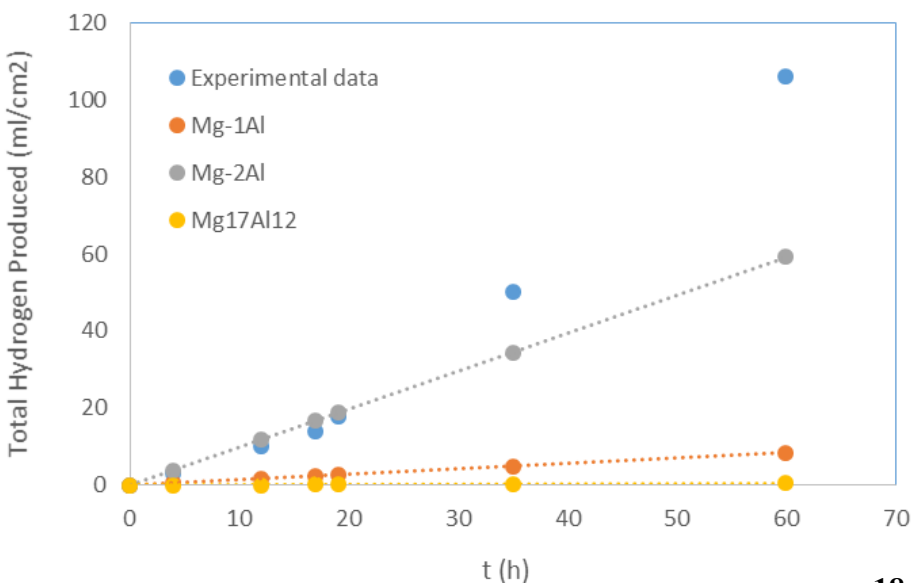
-2.45 eV



-2.40 eV



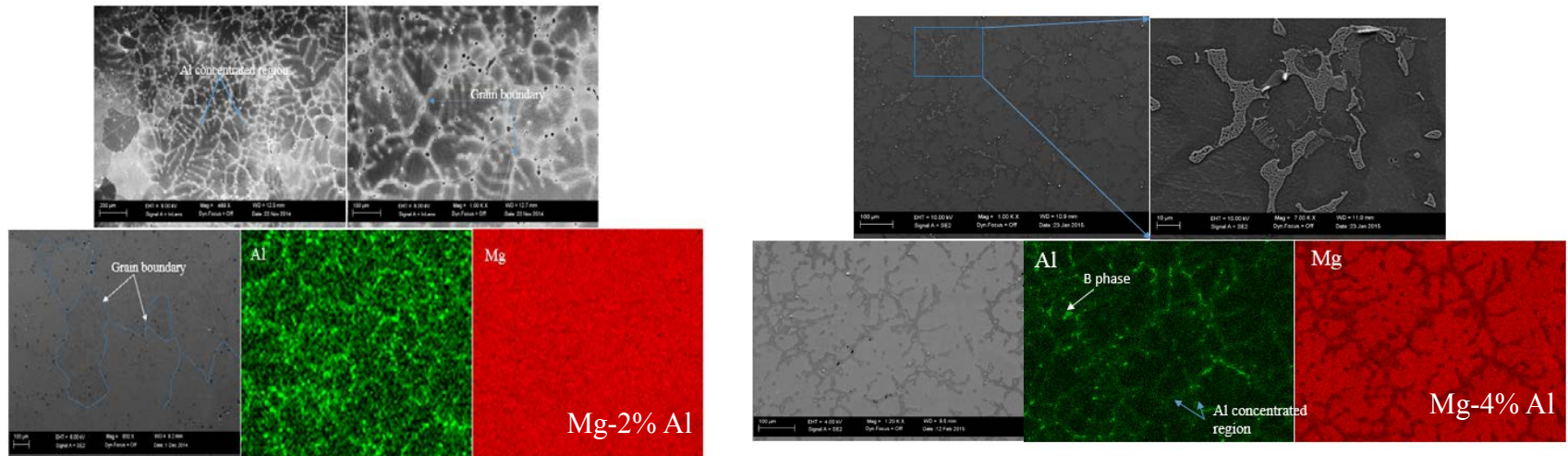
-2.52 eV



The final H₂ evolution rate near cathodic Al-sites and Mg₁₇Al₁₂ decrease – Less corrosion as seen in experiments

Bridging to Microstructural Characteristics of Mg-Al alloys

SEM-EDS element mapping for Mg-2% Al and Mg-6% Al alloy



Materials	grain size (um)	particle size (um)	Particle Number density(mm ²)	NND (um)	Particle type	Matrix type	Mean area of second phase particle (um ²)	Second phase particle area fraction
Pure Mg	1000							
Mg-2% Al	500							
Mg-6% Al	161.25	5.6	1434	13.172	M ₁₇ Al ₁₂	saturated Al	31.368	4.494%

- For Mg-2% Al alloy, no second phase was formed, dendritic arm region and grain boundaries have higher aluminum intensity.
- For Mg-6% Al alloy, Mg₁₇Al₁₂ phase was formed, the second phase mainly distributed along grain boundaries and dendritic arm region.

Outline

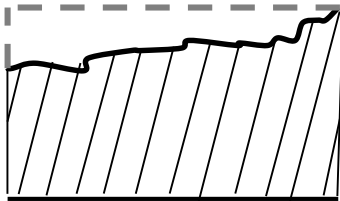
- Corrosion Damage Framework
- Mesoscale Corrosion Modeling
- Nanoscale Corrosion Simulation
- **Experiment Calibration**
- Application and Implementation

General Corrosion Model Calibration

$$\dot{\phi}_{total} = \dot{\phi}_{gc} + \dot{\phi}_{pc} + \dot{\phi}_{ic}$$

General corrosion refers to corrosion dominated by uniform thinning that proceeds without appreciable localized attack

$$\dot{\phi}_{gc} = \frac{C_1 M}{F Z} (C_2 - \phi_{gc})$$



$$C_1 = 10\xi^2 + 70\xi - 250$$

$$C_2 = 47\xi^{-0.075}$$



Faraday's Law of electrolysis summarizes mass loss based on the total electric charge of the substance.

m – mass

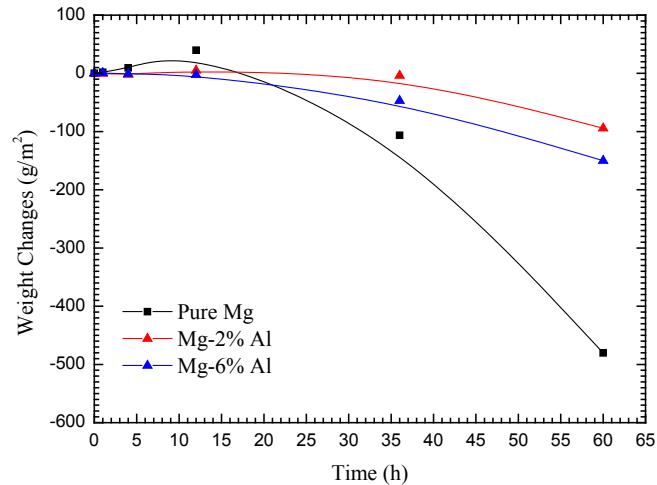
F – Faraday constant

M – the molar mass of the substance

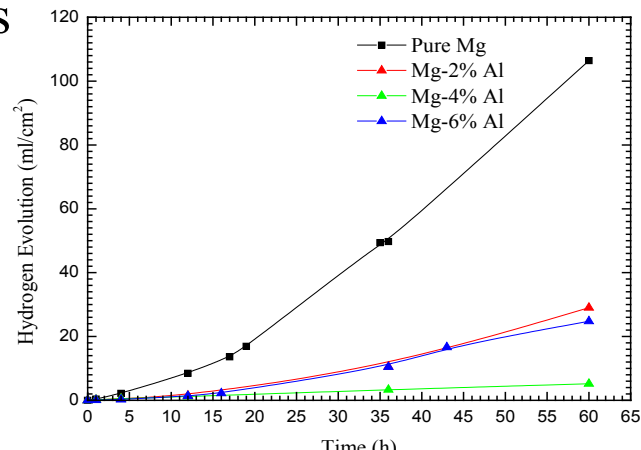
z – the valence number of ions

ξ – Al percentage in the materials

Mass Loss



Hydrogen Evolution Rate



Pitting Corrosion-Nucleation Calibration

$$\dot{\phi}_{pc} = \dot{\eta}_p v_p c_p + \eta_p \dot{v}_p c_p + \eta_p v_p \dot{c}_p$$

The nucleation term is defined as the number density/unit area

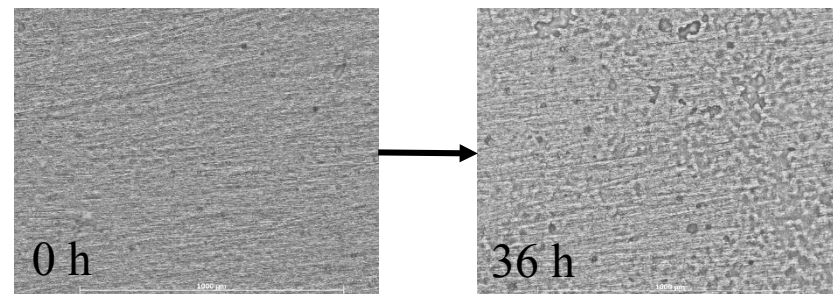
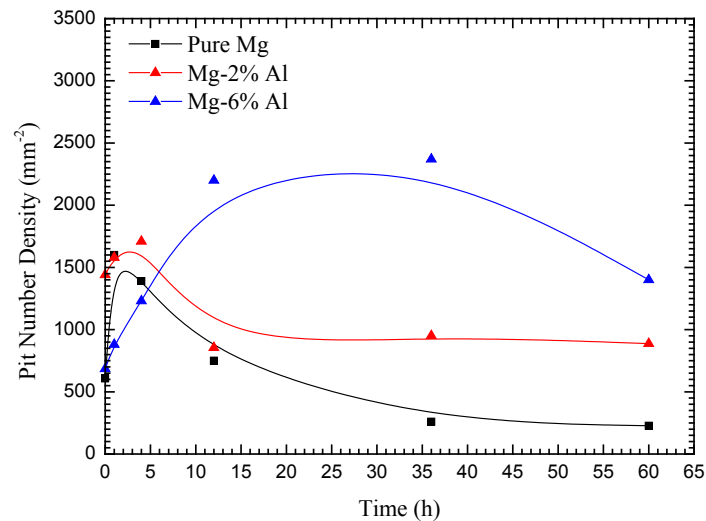
$$\dot{\eta} = \begin{cases} C_3(C_4 - \eta) & \text{if } t < t_{critical} \\ C_5(C_6 - \eta) & \text{if } t \geq t_{critical} \end{cases}$$

$$t_{critical} = 1.1437 e^{0.05253\xi}$$

$$C_3 = 0.17 \ln(\xi) + 0.5344 \quad C_4 = 128.57\xi + 1607.1$$

$$C_5 = -0.0016\xi + 0.0593 \quad C_6 = 741.88\xi^{0.1513}$$

Pit Number Density



where C_3, C_4, C_5, C_6 are material parameters, that are related to material's Al percentage, ξ , in this study, and as a function of second phase/particle volume fraction, particle size, temperature, pH level. $t_{critical}$ is the transition time from pit nucleation dominated to pit coalescence or general corrosion dominated.

Pitting Corrosion-Growth Calibration

$$\dot{\phi}_{pc} = \eta_p v_p c_p + \eta_p \dot{v}_p c_p + \eta_p v_p \dot{c}_p$$

The growth term signifies the pit area at which pits are growing across the surface.

$$\dot{v}_p = \begin{cases} C_7(C_8 - A) & \text{if } t < t_{critical} \\ C_9(C_{10} + A) & \text{if } t \geq t_{critical} \end{cases}$$

$$C_7 = 0.0425e^{0.3214\xi}$$

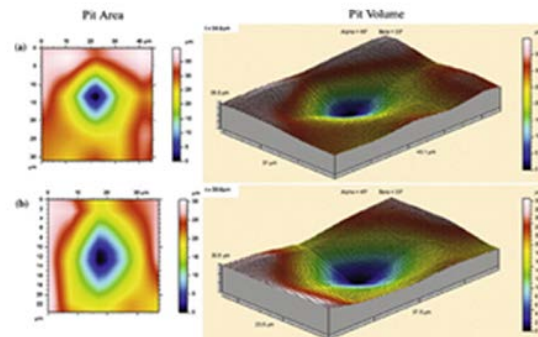
$$C_8 = 253.25\xi + 1533.7$$

$$C_9 = 0.0038\xi^2 - 0.0099\xi + 0.0012$$

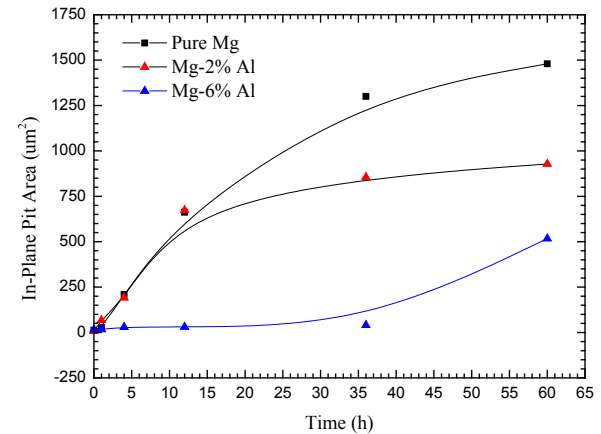
$$C_{10} = 1.2499\xi^2 - 0.4996\xi - 1$$

where C_7, C_8, C_9, C_{10} are material parameters that relate to Al percentage in the materials, also are as a function of temperature, pH level, and materials microstructural characteristics.

A is the average in-plane pit area on the specimen surfaces, please notice that A can also be the average pit volume if you measured pit volume instead of in-plane pit area



In-Plane Pit Area



Pitting Corrosion-Coalescence Calibration

$$\dot{\phi}_{pc} = \dot{\eta}_p v_p c_p + \eta_p \dot{v}_p c_p + \eta_p v_p \dot{c}_p$$

The coalescence rate can be directly related to the nearest neighbor distance of two pits on the surface

$$\dot{NND} = \begin{cases} C_{11}(C_{12}-NND) & \text{if } t < t_c \\ C_{13}(C_{14}-NND) & \text{if } t \geq t_c \end{cases}$$

$$\dot{c}_p = \frac{k_e q_1 q_2}{\epsilon_0 \pi (\dot{NND}(t))^4}$$

k_e is the proportionality constant = $8.987 \times 10 \text{ Nm}^2 / \text{C}^2$

q_1 and q_2 are point charges

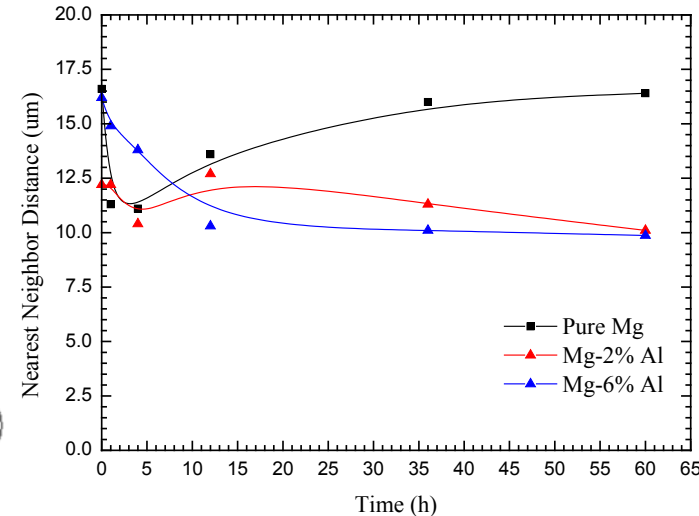
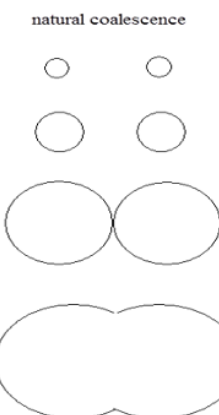
ϵ_0 is the electric constant = $8.854 \times 10^{-12} \text{ F/m}$

NND is the separation distance between pits

\dot{c}_p is the coalescence rate

Coulomb's Law and Maxwell's stress both represent an electrostatic interaction between two charged particles with respect to the force on the body.

Nearest Neighbor Distance



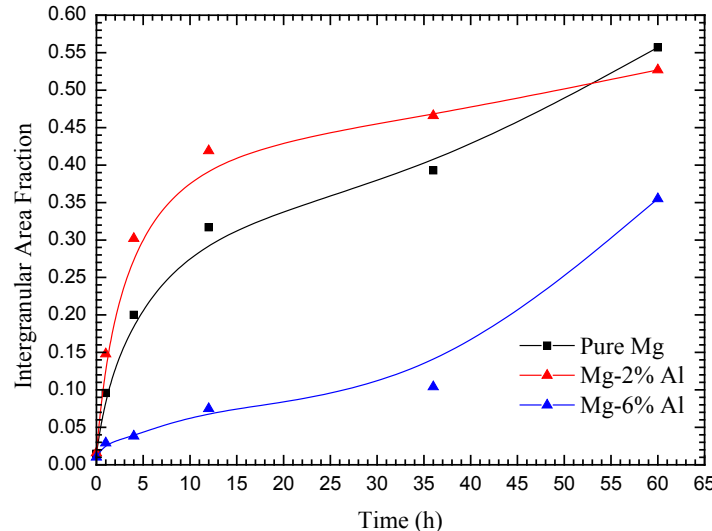
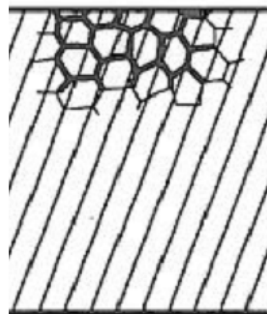
Intergranular Corrosion Calibration

$$\dot{\phi}_{total} = \dot{\phi}_{gc} + \dot{\phi}_{pc} + \dot{\phi}_{ic}$$

Intergranular Corrosion Area Fraction

Intergranular corrosion takes place when the corrosion rate of the grain-boundary areas of an alloy exceeds that of the grain interiors

$$\dot{\phi}_{ic} = \begin{cases} C_{15}(C_{16} - \phi_{ic})\left(\frac{MO}{MO_0}\right)^{z_{ic}} & \text{if } t < t_c \\ C_{17}(C_{18} + \phi_{ic})\left(\frac{MO}{MO_0}\right)^{z_{ic}} & \text{if } t \geq t_c \end{cases}$$



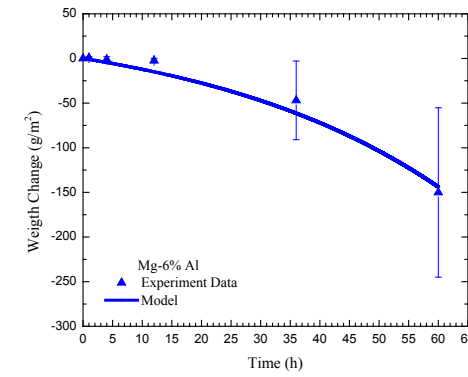
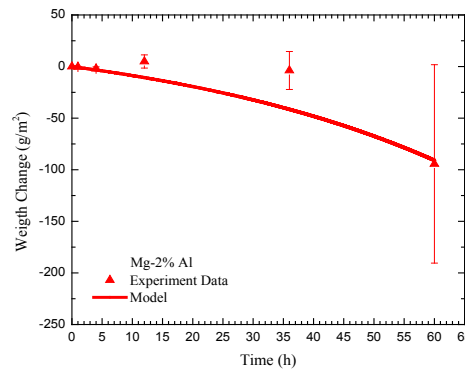
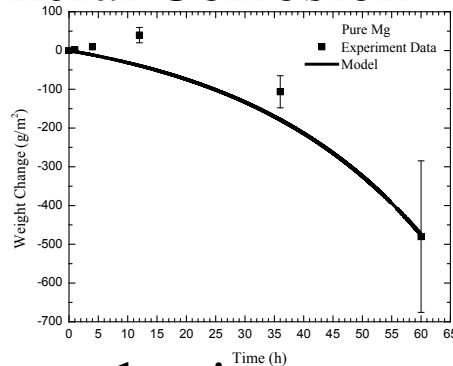
Form of localized corrosion caused by precipitates and segregation leading to the formation of microgalvanic cells, $\left(\frac{MO}{MO_0}\right)^{Z_{ic}}$ is a misorientation factor that represents galvanic cells formed, C_{15} , C_{16} , C_{17} , C_{18} are material parameters

Outline

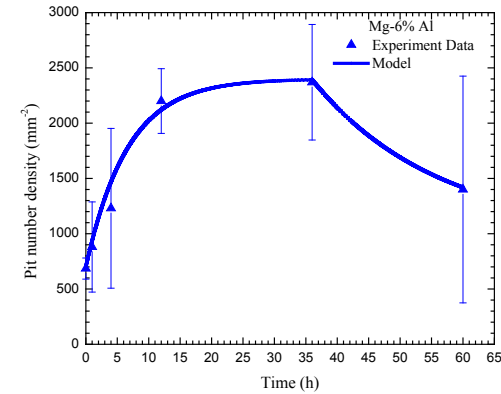
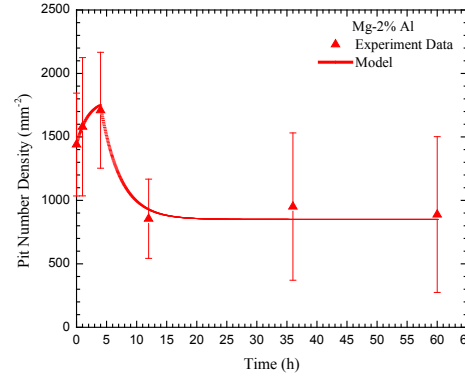
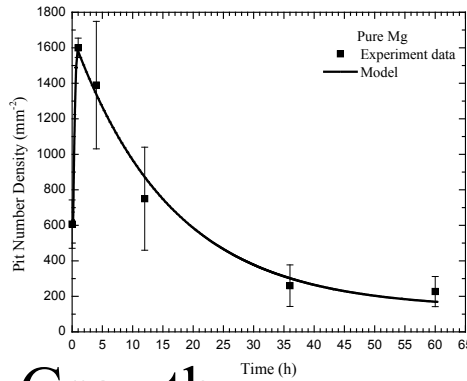
- Macroscale Corrosion Damage Framework
- Mesoscale Corrosion Modeling
- Nanoscale Corrosion Simulation
- Experiment Calibration
- Application and Implementation

Application-Casted Mg alloys in 3.5 wt.% NaCl solution Environment

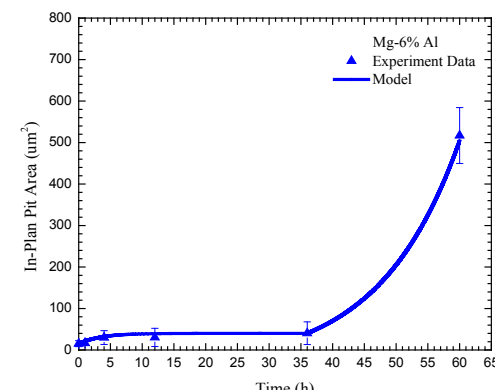
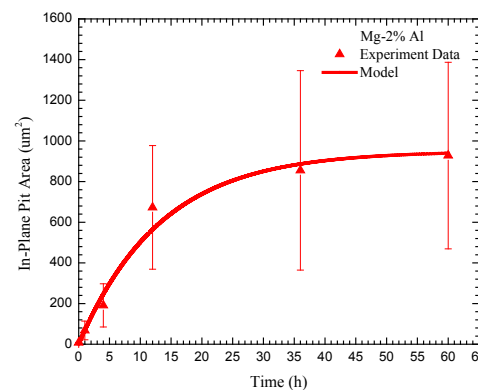
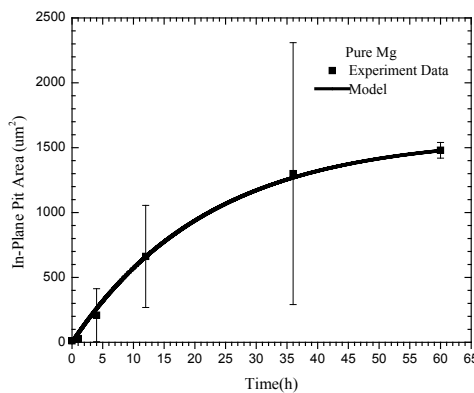
- General Corrosion



- Pit nucleation



- Pit Growth



Summary

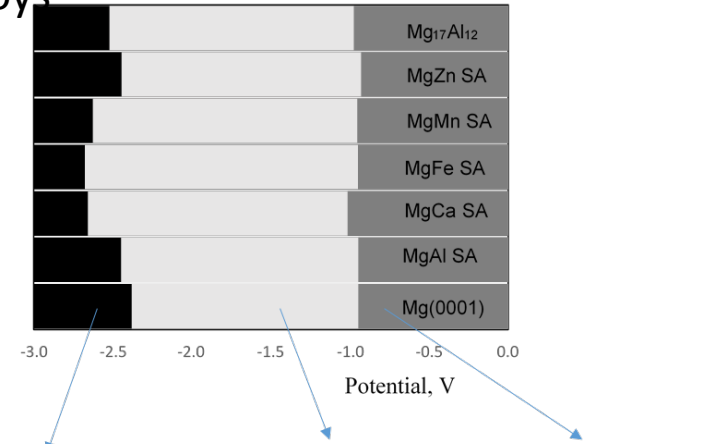
Preliminary Conclusion

- Developed a fully coupled ISV model that captures the corrosion damage evolution for magnesium alloys
- Bridged information passage from different length scale
- Completed corrosion calibration experiments for Mg-Al alloys
- Qualitative agreement with DFT that pure Mg H-evolution is greater compared to Mg-Al
- Anodic dissolution of Mg-X can be organized with respect to the baseline with Mg-Ca seems least reactive towards H-evolution according to DFT

Next Steps

- Implementation of model to Mg-Zn magnesium alloys
- Mg-Zn magnesium alloys model calibration
- Connect the limiting current density at different overpotentials to include galvanic effects where, overpotential ($\varepsilon_V - \varepsilon_{o,V}$) and H-coverage ratios (θ_H / θ_H^0) obtained from DFT are related below in a Butler-Volmer form

$$i_k = i_{0,V} \left\{ \frac{\theta_H}{\theta_H^0} \exp \left[\frac{\alpha F}{RT} (\varepsilon_V - \varepsilon_{o,V}) \right] - \frac{1-\theta_H}{1-\theta_H^0} \exp \left[\frac{-(1-\alpha)F}{RT} (\varepsilon_V - \varepsilon_{o,V}) \right] \right\}$$



Change with Potential from DFT